Docosahexaenoic acid slows inflammation resolution and impairs the quality of healed skin tissue

Thamiris Candreva[1*], Carolina M.C. Kühl[1*], Beatriz Burger[1], Mariah B.P. dos Anjos[1], Márcio A. Torsoni[2], Sílvio R. Consonni[3], Amanda R. Crisma[4], Helena L. Fisk[5], Philip C. Calder[5,6], Felipe C.P. de Mato[7], Erica M. Sernaglia[7], Marco A.R. Vinolo[7], Hosana G. Rodrigues[1★]

[1]Laboratory of Nutrients and Tissue Repair, School of Applied Sciences, University of Campinas, Limeira/SP, Brazil, [2]Laboratory of Metabolic Disorders, School of Applied Sciences, University of Campinas, Limeira/SP-Brazil, [3]Department of Biochemistry and Tissue Biology, Institute of Biology, University of Campinas, Campinas/SP, Brazil, [4]Department of Physiology and Biophysics, University of São Paulo, São Paulo/SP-Brazil, [5]Human Development and Health, Faculty of Medicine, University of Southampton, Southampton, UK, [6]NIHR Southampton Biomedical Research Centre, University Hospital Southampton NHS Foundation Trust and University of Southampton, Southampton, UK, [7]Department of Genetics, Evolution, Microbiology and Immunology, Institute of Biology, University of Campinas, Campinas/SP, Brazil

* These authors equally contributed to the manuscript.

★ Corresponding author: Hosana Gomes Rodrigues

Address: School of Applied Sciences/UNICAMP

Rua Pedro Zaccaria, 1300 Limeira/SP/Brazil

CEP: 13485-350

e-mail: hosanagr@unicamp.br

ABBREVIATIONS LIST

omega-3 (ω-3), fatty acids (FA), wild-type (WT), docosahexaenoic acid (DHA), myeloperoxidase (MPO), interleukin-10 (IL-10), eicosapentaenoic acid (EPA), phosphate-buffered saline (PBS), standard deviation of mean (SD), arachidonic acid (AA), phosphatidylcholine (PC), phosphatidylethanolamine (PE), docosapentaenoic acid (DPA), chemokine (C-X-C motif) ligand-1 (CXCL-1), tissue inhibitor of metalloproteinase-1 (TIMP-1), vascular-endothelial growth factor (VEGF), tumor necrosis factor-alpha (TNF-α), alpha-linolenic acid (ALA), eicosatetraenoic acid (ETA), lipopolysaccharide (LPS), 5-lipoxygenase (5-LOX), epidermis (E), dermis (D), granulation tissue (GT), A9-oxo-11R,15S-dihydroxy-5Z,13E-prostadienoic acid (**PGE2**); 9S,15S-dihydroxy-11-oxo-5Z,13E-prostadienoic acid (**PGD2**); 9,15-dioxo-11R-hydroxy-5Z-prostenoic acid (**dhkPGE2**); 11S-hydroxy-5Z,8Z,11E,14Z-eicosatetraenoic acid (**11-HETE**); 9S,11R,15S-trihydroxy-5Z,13E-prostadienoic acid-cyclo [8S,12R] (**8-iso-PGF2Aiii**); 9-hydroxy-5Z,7E,11Z,14Z-eicosatetraenoic acid (**9-HETE**); 5S-hydroxy-6E,8Z,11Z,14Z-eicosatetraenoic acid (**5-HETE**); 15S-hydroxy-5Z,8Z,11Z,13E-eicosatetraenoic acid (**15-HETE**); 8S-hydroxy-5Z,9E,11Z,14Z-eicosatetraenoic acid (**8-HETE**); 12S-hydroxy-5Z,8Z,10E,14Z-eicosatetraenoic acid (**12-HETE**); 12-oxo-5Z,8Z,10E,14Z-eicosatetraenoic acid (**12-oxo-ETE**); 19(20)-epoxy-4Z,7Z,10Z,13Z,19Z-docosapentaenoic acid (**19(20)EpDPE**); 11-hydroxy-5Z,8Z,12E,14Z,17Z-eicosapentaenoic acid (**11-HEPE**); 13-hydroxy-4Z,7Z,10Z,14E,16Z,19Z-docosahexaenoic acid (**13-HDoHE);** 5-hydroxy-6E,8Z,11Z,14Z,17Z-eicosapentaenoic acid (**5-HEPE**); 7-hydroxy-4Z,8E,10Z,13Z,16Z,19Z-docosahexaenoic acid (**7-HDoHE**); 4-hydroxy-5E,7Z,10Z,13Z,16Z,19Z-docosahexaenoic acid (**4-HDoHE**); 15-hydroxy-5Z,8Z,11Z,13E,17Z-eicosapentaenoic acid (**15-HEPE**); 11-hydroxy-4Z,7Z,9E,13Z,16Z,19Z-docosahexaenoic acid (**11-HDoHE);** 18-hydroxy-5Z,8Z,11Z,14Z,16E-eicosapentaenoic acid (**18-HEPE**); 16(17)-epoxy-4Z,7Z,10Z,13Z,19Z-

docosapentaenoic acid (**16(17)EpDPE);** 19,20-dihydroxy-4Z,7Z,10Z,13Z,16Z-docosapentaenoic acid (**19(20)DiHDPA**), fatty acid methyl esters (FAMEs), hexadecyltrimethylammonium (HTAB), helium (He), intraperitoneal (i.p), fetal bovine serum (FBS).

PERSPECTIVES

- Wound healing is an immune process evolutionarily conserved and essential for life maintenance. Inflammation is the first event that occurs and it needs to be contained for optimal tissue repair. However, several factors, including the diet, modulate inflammatory parameters contributing to better or worse healing. ω-3 fatty acids are able to modulate inflammatory responses.
- To understand their role in tissue repair, here we evaluated endogenously produced and orally supplemented ω-3 fatty acids, during cutaneous wound healing.
- The major finding is that the increase in ω-3 fatty acids inhibited the resolution of inflammation and impaired the quality of the healed tissue, suggesting a deleterious effect on wound healing.

ABSTRACT

There is no consensus on the effects of omega-3 (ω-3) fatty acids (FA) on cutaneous repair. To solve this problem, we used 2 different approaches: 1) *FAT-1* transgenic mice, capable of producing endogenous ω-3 FA; 2) wild-type (WT) mice orally supplemented with DHA-enriched fish oil. *FAT-1* mice had higher systemic (serum) and local (skin tissue) ω-3 FA levels, mainly docosahexaenoic acid (DHA), in comparison to WT mice. *FAT-1* mice had increased myeloperoxidase (MPO) activity and content of CXCL-1 and CXCL-2, and reduced IL-10 in the skin wound tissue three days after the wound induction. Inflammation was maintained by an elevated TNF-α concentration and presence of inflammatory cells and edema. Neutrophils and macrophages isolated from *FAT-1* mice, also produced increased TNF-α and reduced IL-10 levels. In these mice, the wound closure was delayed, with a wound area 6-fold bigger in relation with WT group, on the last day of analysis (14 days post-wounding). This was associated with poor orientation of collagen fibers and structural aspects in repaired tissue. Similarly, DHA group had a delay during late inflammatory phase. This group had increased TNF-α content and $CD45^{+}F4/80^{+}$ cells at the 3rd day after skin wounding and increased concentrations of important metabolites derived from ω-3, like 18-HEPE and reduced concentrations of those from ω-6 FA. In conclusion, elevated DHA content, achieved in both *FAT-1* and DHA groups, slowed inflammation resolution and impaired the quality of healed skin tissue.

Keywords: omega-3 fatty acids, cytokines, wound healing

INTRODUCTION

Chronic wounds are a global health problem, especially for obese, diabetic and elderly individuals [1].

The inflammatory response is a critical step for effective tissue repair: an imbalance between pro- and anti-inflammatory mediators maintains the wound in a prolonged state of inflammation; limiting its closure and therefore extending the healing process [2].

The inflammatory phase of the wound healing is divided into initial and late responses [3]. The initial inflammatory response involves an increase in vascular permeability to facilitate migration of neutrophils and macrophages; an increase in phagocytosis that aims to clean the injured site; and the production of cytokines and chemokines that amplify the migration of inflammatory cells and orchestrate the synthesis of new tissue [4-5]. On the other hand, the late response is characterized by an increase in the production of pro-resolving molecules such as interleukin-10 (IL-10) and fatty acid-derived lipid mediators that will orchestrate a reduction in pro-inflammatory markers [4-5].

The ω-6 and ω-3 FA families have been described as modulators of inflammation [6-7]. ω-3 FAs, such as eicosapentaenoic acid (EPA; 20:5ω-3) and DHA (22:6ω-3), have anti-inflammatory effects, acting through to changes in production of cytokines, cellular metabolism, expression of pro-inflammatory genes and angiogenesis [7]. The inhibition of inflammation by ω-3 FAs has been reported in several inflammatory diseases, such as cardiovascular [8], obesity [9], diabetes [10], neurological [11] and cancer [12], but their effects on wound healing are not clear yet [6]. Some authors reported that supplementation of rodent chow with ω-3 FAs inhibits skin wound healing [13] but others described no effect [14]. Topical use of ω-3 FAs has been linked with an increased rate of wound closure [15]. The discrepancies among these findings may be associated with the absolute amount of ω-3 FAs used or in the relative abundance of the two-main bioactive ω-3 FAs, EPA and DHA.

These two ω-3 FAs do not have the same effects as reported in several experimental and clinical conditions [16-17].

Considering the anti-inflammatory actions of ω-3 FAs, we aimed to investigate the effect of increased skin content of DHA on the inflammatory phase of cutaneous wound healing. Two experimental models were used: *FAT-1* transgenic mice and C57Bl/6 mice supplemented with DHA-rich fish oil. *FAT-1* transgenic mice convert ω-6 into ω-3 FAs and were generated by the insertion of *fat-1* gene from the nematode *Caenorhabditis elegans* into their genome [18].

EXPERIMENTAL

Mice and treatment

All animal study protocols were approved by the Ethics Committee (CEUA – 4175-1 and 4122-1) and by the Biosafety Internal Committee (CiBIO – 370) of the School of Applied Sciences/UNICAMP. All the experiments with animals were performed at the School of Applied Sciences/UNICAMP/Brazil. The studies were conducted according to the NIH Guide for the Care and Use of Laboratory Animals.

Adult (2 months of age) male *FAT-1* transgenic mice and their non-transgenic littermate WT controls were used. All mice received a standard commercial diet. Adult (2 months of age) male C57Bl/6 mice were supplemented with DHA-rich oil (25 µL/day) or water as control in the same volume, given by oral gavage once daily for 4 weeks. After this period of time, skin wound was induced, and the supplementation was maintained until to the collection of wound tissue. Mice were kept in a light/dark cycle of 12 hours at a temperature of 23 ± 2 °C.

To better understand if the effects observed were due to the increase in DHA or due to the decrease in ω-6 fatty acids, mainly linoleic acid (LA), we supplemented mice with a mixture of DHA-rich oil+ pure LA (25 µL/day) given by oral gavage once daily for 4 weeks.

Determination of DHA-rich oil composition

Methanolic NaOH (1 mL) was added to 150 uL of DHA-rich oil and heated for 10 minutes. After cooling, 2 mL of esterification reagent was added to the sample and heated for 5 minutes. Then, 2 ml of isoctane and 5 ml of saturated NaCl solution were added. After separation of the phases, the upper phase was aspirated. Chromatographic analyses were performed using a gas chromatograph-mass spectrometer (model GCMS-QP2010 Ultra; Shimadzu), and a fused-silica capillary Stabilwax column (Restec Corporation, U.S.) with dimensions of 30 m × 0.25 mm internal diameter (i.d) coated with a 0.25-µm thick layer of

polyethylene glycol. The initial oven temperature was 80 °C, which was increased to 175 °C at a rate of 5 °C/min and, finally, the temperature was increased up to 230 ºC at a rate of 3 °C/min (hold 13 min). Sample volumes of 1 µl were injected at 250 °C using a split ratio of approximately 25:1. High-grade pure helium (He) was used as the carrier gas with a constant flow rate of 1.0 mL/min. Mass conditions were as follows: ionization voltage, 70 eV; ion source temperature, 200 ºC; full scan mode in the 35–500 mass range with 0.2 s/scan velocity.

Genotyping

To identify the *FAT-1* transgenic mice, DNA was extracted from 5 mm of the mouse tail.

Tail tissue was digested in 200 uL of lysis buffer with proteinase K overnight at 50°C and then 200 uL of lysis buffer without proteinase K were added. After 20 min of centrifugation, supernatant was collected and 500 uL of ethanol were added. Samples were centrifuged for 10 min and pellets were re-suspended in 40 or 80 uL of Tris EDTA buffer (pH 7.5-8.0) and incubated for 30 min at 65 °C. For PCR assay, 50 ng/uL of extracted DNA were used. The PCR reaction mix contained: 2.5 uL of buffer (Invitrogen, Carlsbad, CA), 1.5 uL of 50 mM $MgCl_2$ 50 mM (Invitrogen), 0.5 uL of 10 mM DNTP (Invitrogen), 0.5 uL of sense primer (5'-ACCAACTGTGGATGCTTTCC-3') (Invitrogen), 0.5 uL of anti-sense primer (5'-GCATTGCTTCCCAATCCTTA-3') (Invitrogen), 0.1 uL of platinum TaqDNA polymerase (Invitrogen) and 17.4 uL of RNA free water. The thermocycler program consisted of: 3 min at 94°C followed by 40 cycles of 30 sec at 95°C, 1 min at 60°C, 1 min at 72°C and then 10 min at 72°C and 10°C to cool the samples. Amplified PCR products were run through a 1.5 % agarose gel with 5 uL of Sybr Safe DNA gel stain (Invitrogen) (**Supplemental Figure 1**).

Skin wound induction and serum collection

Mice were anesthetized with xylazine and ketamine (1:2 vol/vol) and an area of 10 mm^2 of skin from the lumbar region was shaved and then removed by surgery. After wound

induction, skin tissues were collected at specified time points. The skin tissues were homogenized following a protocol previously described [19].

Blood was collected from the heart and kept at room temperature for 1 hour to clot. Blood was then centrifuged at 3,500 rpm for 5 minutes and the supernatant (serum) collected.

Determination of serum and skin tissue fatty acid composition

Lipid from serum and from homogenized skin was extracted using chloroform:methanol (2:1 vol/vol) as already described [20].

Lipids from skin tissues were separated into the major phosphatidylcholine (PC) and phosphatidylethanolamine (PE) fractions using solid-phase extraction on aminopropylsilica cartridges. Fatty acid methyl esters (FAMEs) were produced by incubation with methanol containing 2% (vol/vol) H_2SO_4 at 50°C for 2 hr. After letting the tubes to cool down, samples were neutralized with a solution of 0.25 M $KHCO_3$ and 0.5 M K_2CO_3. FAMEs were extracted into hexane, dried down, redissolved in a small volume of hexane. FAMEs were separated by gas chomatography on an Agilent 6890 gas chromatograph under the conditions described previously [20]. FAMEs were identified by comparison with run times of authentic standards. For skin tissue data are expressed as percentage contribution to total fatty acids, as FAMEs, in the sample. For serum, data are expressed as absolute concentration.

Analysis of wound closure

Skin wounds were photographed daily with a Sony cyber shot digital camera (DSC-S950S 10MP 4X optical zoom). After scanning the images, the wound area was measured using Image J software. Results are expressed as percentage (%) of the original wound area.

Cytokines, chemokines and growth factors in skin tissue

Unwounded and wounded skin tissues were homogenized in phosphate-buffered saline (PBS) containing protease inhibitor (Roche Diagnostics, Mannheim, Germany). After homogenization, samples were centrifuged, and the supernatant collected. IL-1β, IL-6, IL-10,

TNF-α, CXCL-1, CXCL-2, TIMP-1 and VEGF concentrations were determined by ELISA as previously described [21] using the Duo Set kit (R&D System, Minneapolis, MN, USA). The results were normalized to the amount of protein in the tissue homogenate determined using the method of Bradford [22].

MPO activity in skin wound tissue

Skin wound tissues were homogenized in potassium phosphate buffer (50 mM), pH 6.0 containing 0.5% hexadecyltrimethylammonium (HTAB) (Sigma Aldrich, ≥98%), and then centrifuged at 12,000 rpm for 10 min. Aliquots of supernatants (10 uL) were added to 96 well plates along with potassium phosphate buffer, o-dianisidine and 20 mM hydrogen peroxide. The activity was determined by measuring the absorbance at 450 nm. The results were normalized to the amount of protein in the tissue homogenate determined using the method of Bradford [22].

Skin tissue histology

Skin samples were collected and fixed in formaldehyde (4% diluted in 0.1 M PBS (pH 7.4)) for 24 h at 4°C. The tissues were dehydrated in graded concentrations of alcohol, embedded in paraffin and sectioned transversely at a width of 5 μm. Serial sections were mounted on slides and stained with H&E and Sirius Red using a protocol previously described [23]. The sections were then examined and imaged using a Leica stereoscopic microscope (MZ10F) coupled with a Leica camera (DFC310 FX) and an Olympus microscope (U-LH100HG) with images representative of the histological structures registered in digital image capture and analysis system (Camera: Olympus / U-TVO.63XC / T2).

Tissue collagen deposition was detected by Sirius Red staining combined with polarized light detection. Briefly, the slides were incubated with Sirius Red solution dissolved

in aqueous saturated picric acid for 1 hour, washed in tap water, incubated for 15 minutes in hematoxylin, dehydrated and mounted.

Eicosanoids in skin tissue

All solvents were of chromatography purity. Eicosanoids used for primary standards in standard curves as well as their deuterated analogs were from Cayman Chemicals (Ann Arbor, MI) and Biomol (Enzo Life Science, Framingdale, NY).

Eicosanoid extraction: For extraction, 100 mg of skin wound tissue were supplemented with a cocktail consisting of 26 deuterated internal standards and purified by solid phase extraction on Strata-X columns (Phenomenex, Torrance, CA) following the activation procedure provided by the distributor. Samples were eluted with 1 ml of 100% methanol, the eluent was dried under vacuum and dissolved in 50 µl of buffer A consisting of water/acetonitrile/acetic acid (60/40/0.02, vol/vol/vol) and immediately used for analysis.

Reverse-phase liquid chromatography and mass spectrometry: Eicosanoids were analyzed as previously described [24-25]. Briefly, eicosanoids were separated by reverse phase chromatography using a 1.7 um, 2.1 mm x 100 mm BEH Shield Column (Waters, Milford, MA) and an Acquity UPLC system (Waters, Milford, MA). The column was equilibrated with buffer A and 5 µl of sample was injected via the autosampler. Samples were eluted with a step gradient to 100% buffer B consisting of acetonitrile/isopropanol (50:50, vol/vol). The liquid chromatography effluent was interfaced with a mass spectrometer and mass spectral analysis was performed on an AB SCIEX 6500 QTrap mass spectrometer equipped with an IonDrive Turbo V source (AB SCIEX, Framingham, MA). Eicosanoids were measured using multiple reaction monitoring (MRM) pairs with the instrument operating in the negative ion mode. Collisional activation of the eicosanoid precursor ions was achieved with nitrogen as the collision gas, and the eicosanoids were identified by

matching their MRM signal and chromatographic retention times with those of pure identical standards.

Quantification of eicosanoids: Eicosanoids were quantified by the stable isotope dilution method. Briefly, identical amounts of deuterated internal standards were added to each sample and to all the primary standards used to generate standard curves. To calculate the amount of eicosanoids in a sample, ratios of peak areas between endogenous eicosanoids and matching deuterated internal eicosanoids were calculated. Ratios were converted to absolute amounts by linear regression analysis of standard curves generated under identical conditions.

Cell types in skin tissue

Skin tissue was collected and washed twice in PBS, cut into small pieces with scissors and dissociated by enzymatic digestion. The resulting cell suspension (1 x 10^6 cells) was washed twice with PBS containing 1% albumin and re-suspended in 100 μL of this buffer. Anti-CD45-FITC, anti-F4/80-APC-Cy7, anti-Ly6G-PE and anti-CD4-APC conjugated antibodies were added to the suspension (1:10) and the cells were incubated at 4°C for 15 minutes protected from light. Negative control cells were incubated with non-reactive labelled IgG antibody. After this period, the cells were washed twice with PBS and analysed with a BD-FACS Accuri flow cytometer (Becton Dickinson). The fluorescence was determined by the specific filter for each fluorochrome. One hundred thousand events were acquired per sample. Histograms were analyzed using BD Accuri software (BD Bioscience, Maryland, USA).

Obtaining intraperitoneal cells

Six hours after intraperitoneal (i.p) inoculation of 1 mL thioglycollate 4%, WT and *FAT-1* mice were euthanized and to obtain the intraperitoneal lavage, 5 mL of PBS was used, and the region was massaged for cell detachment. Cells were

centrifuged (2,000 rpm for 10 minutes at 4 °C), resuspended in 5 mL of lysis solution and centrifuged one more time. The supernatant was discarded, and the cells resuspended in 1 mL of RPMI medium + 10% of fetal bovine serum (FBS). From this resuspension 20 uL were used for cytocentrifuge slides and 0.5 x 10^6 cells were labeled for cytometry (counting in Neubauer's chamber) (**Supplemental Figure 2A**). One of the groups was labeled with anti-Ly6G-APC and CD11b-PE and the other group with F4/80-APC and CD11c-PE, plus a negative control sample (absent antibody). In both cases the antibodies were diluted 10x. After 15 minutes incubation under light, the samples were read on the Verse cytometer (BD Bioscience, Maryland, USA).

Cells isolation from bone marrow and neutrophil culture

Cells of hind paws from WT and *FAT-1* mice were used. After washing the tibia and femur bones with 5 mL of HBSS 1X, the cells were collected by centrifugation (1,200 rpm for 10 minutes at 4°C) and re-suspended in 3 mL of HBSS 1X. Two gradients of Percoll (Ge Healthcare Bio-Sciences AB) (65% and 55%) were prepared, which were joined in a conical tube, with the 65% gradient placed below the 55% gradient and the cells were layered on top of the upper gradient. The sample was then centrifuged at 2,400 rpm for 30 minutes at 4°C, with no brake used during deceleration. Two bands were visible: the first band included the mononuclear cells, which was used for macrophage differentiation with the 55% Percoll gradient, while the second band included the polymorphonuclear cells, containing neutrophils, which were removed and transferred to a conical tube containing 30 mL of PBS for washing. Cells were collected by centrifugation at 2,000 rpm for 10 minutes at 4°C. The cells were re-suspended in 2 mL RPMI medium containing fetal bovine serum (10%). Neutrophils were plated (0.6 x 10^6 cells/mL) and the supernatant collected after 6 hours (**Supplemental Figure 2D**). Cytokines were measured by ELISA and for phagocytosis (not shown), bacteria (*Escherichia coli*) were maintained in contact with the neutrophils for 2 hours, having an MOI

of 1:50. Neutrophils were labeled with anti-Ly6G-APC and read on the Verse cytometer (BD Bioscience, Maryland, USA).

Macrophage isolation and culture

Cells were collected from the peritoneal cavity of WT and *FAT-1* mice 72 hours after injection of sterile thioglycollate solution (4%). All cells were plated (1 x 10^6 cells/mL) and incubated at 37°C for 24 hours. Subsequently, non-adherent cells were removed by washing the plates with PBS and adherent cells were incubated in the presence or absence of l μg/mL LPS for 24 hours. At the end of the incubation period, cell supernatant was collected and used for cytokine analysis by ELISA (**Supplemental Figure 3A**) and for NO analysis (not shown).

Statistics

Results are presented as mean ± standard deviation of mean (SD). Comparisons between groups were performed using Student's t-test or two-way ANOVA using the Prism 7.0 software (GraphPad Software, Inc., San Diego, CA, USA). Differences were considered significant for $p < 0.05$.

RESULTS

FAT-1 mice have higher levels of DHA in unwounded skin tissue and no alteration in the basal inflammatory state

In unwounded skin tissue, collected at the moment of wound induction, *FAT-1* mice had a lower percentage of arachidonic acid (AA) in phosphatidylcholine (PC) and phosphatidylethanolamine (PE) and higher levels of ω-3 FAs such as docosapentaenoic acid (DPA; 22:5ω-3) and DHA in relation to WT mice (**Figures 1A and 1B**). FAT-1 mice had a 50% lower ω-6/ω-3 ratio in relation to the WT group (**Figure 1C**). These effects did not alter the basal concentrations of inflammatory mediators (**Figure 1D**).

FAT-1 mice had slowed inflammation resolution but no remarkable change in wound closure time

A well-established cutaneous wound healing protocol was used [19,21]. *FAT-1* and WT mice were followed for 14 days after skin wound induction. Throughout this period, *FAT-1* mice had a delay in wound healing. At the 3rd day, the wound area in *FAT-1* mice was 34.6% larger than in the WT group and the delay in wound closure remained until the 14th day post- wound induction. At the 12th day, the open wound area in *FAT-1* mice was 3-fold bigger and at the 14th day it was 6-fold bigger than that observed in the WT group (**Figures 2A and 2B**). No signs of wound infection were observed in the experimental groups during the protocol.

Taken together, these results indicate that, in *FAT-1* mice, there is a modulation in the wound healing process.

FAT-1 mice had prolonged the late inflammatory phase of tissue repair

Infiltration of leukocytes into skin wound tissue was estimated by MPO activity. *FAT-1* and WT mice did not exhibit any difference in skin MPO activity or in skin content of cytokines and chemokines one day after skin wounding (**Figures 3A and 3B**). However, the

FAT-1 mice exhibited a more intense inflammatory state in the skin wound tissue at three days after wound induction as compared with WT mice: increased MPO activity (**Figure 3C**) and higher levels of pro-inflammatory mediators (IL-6, chemokine (C-X-C motif) ligand-1 (CXCL-1), CXCL-2, tissue inhibitor of metalloproteinase-1 (TIMP-1) and vascular-endothelial growth factor (VEGF)) were seen in *FAT-1* mice along with lower IL-10 concentrations than the WT group (**Figure 3D**). The alteration in inflammatory markers of the late inflammatory phase was also seen as elevated concentrations of tumor necrosis factor-alpha (TNF-α) in skin wound tissue collected five days after wound induction (**Figure 3E**). Also at this time point, *FAT-1* mice showed greater presence of inflammatory cells than WT mice. There was a characteristic edema with extravasation of cells and fluid water in the interstitium in *FAT-1* mice (**Figure 3F**).

All these data support the hypothesis that *FAT-1* mice have a disturbed wound healing process due to a prolonged inflammatory response.

Mice supplemented with DHA-rich fish oil phenocopied the *FAT-1* mice responses

In serum and skin wound tissue collected three days after wound induction, *FAT-1* mice had a lower AA (40% in serum, 60% and 49% in skin PC and PE, respectively) and higher DHA (17% in serum, 37% and 34% in skin PC and PE, respectively) than the WT mice. Also, higher concentrations of alpha-linolenic acid (ALA; 18:3ω-3) (39%) and EPA (61%) were observed in serum from *FAT-1* mice, resulting in a lower ω-6/ω-3 ratio compared with the WT group (around 33% lower). *FAT-1* mice also presented higher DPA in PC (76%) and PE (74%) and eicosatetraenoic acid (ETA; 20:4ω-3) (58%) in PE, resulting in a lower (55%) ω-6/ω-3 ratio in both lipid fractions in relation to the WT group (**Figures 4A to 4F**).

Since we found higher DHA concentrations in *FAT-1* mice in relation to WT mice in different biological samples (serum, skin unwounded and skin wound), we hypothesized that the effects on wound healing observed in *FAT-1* mice could be due to the elevation of this

fatty acid. To test this hypothesis, we evaluated the wound healing process in C57Bl/6 mice orally supplemented with DHA-rich oil (more than 60% of DHA) (**Figure 4G and Supplemental Table 1**). Since this represents an increment of only 0.5% in the caloric intake of mice, the dose of DHA-rich oil administrated did not change body weight, water or food consumption of the mice as expected (**Supplemental Figure 4**).

Skin wound induction was performed after 4 weeks of DHA-rich fish oil supplementation and serum was collected three days after wound induction. In these serum samples, we observed higher DHA concentration (24% higher) and less AA (28% lower) in the DHA group than in the control mice (**Figures 4H and 4I**). These alterations resulted in a reduction of 28% in ω-6/ω-3 ratio in the DHA group (**Figures 4J**). DHA-rich fish oil supplementation also increased the incorporation of ω-3 and reduced the ω-6 FA content in unwounded skin tissue (**Supplemental Figure 5**).

In accordance with the data described for the *FAT-1* mice, DHA supplementation modulated cutaneous wound healing: greater wound area was observed between the 3rd and the 10th days after skin wound induction compared to the control mice (**Figures 5A and 5B**).

Next, we analysed the skin inflammatory status in DHA-supplemented mice. No effect of DHA administration was observed on the inflammatory markers analysed either in skin unwounded tissue or in skin wound tissue of one day after wounding (**Supplemental Figures 6A to 6C**). However, at the third day, there was higher TNF-α concentration in skin wound from DHA-fed mice (**Figure 5C**), and this result was maintained until the 7th day after wound induction, indicating a prolongation of the inflammatory phase in these animals (**Figure 5D**).

DHA treatment increased the percentage of macrophages ($CD45^{+}F4/80^{+}$) present in the wound three days after wound induction, when compared to control mice (**Figure 5E**). At the same time, DHA group increased metabolites derived from ω-3 FA. There was an increase in the concentrations of 11-HEPE, 13-HDoHE, 5-HEPE, 7-HDoHE, 4-HDoHE, 15-HEPE,

11-HDoHE, 18-HEPE, 16,17-EpDPE, 19,20-DiHDPE and 19,20-EpDPE. The supplementation with DHA-rich oil also resulted in reduction in AA-metabolites such as: PGE_2, PGD_2, $dhkPGE_2$, 11-HETE, 8-iso-PGF2a, 9-HETE, 5-HETE, 15-HETE, 8-HETE, 12-HETE and 12-oxo-ETE. Nevertheless, although DHA-fed mice had increased concentrations of ω-3 FA-derived metabolites, the concentration of metabolites derived from AA was up to thirty times greater in skin wound tissue, in relation to the concentration of the ω-3 FA-derived metabolites (**Figure 5F**). The concentrations of specialized pro-resolving mediators, such as maresins and resolvins were below the limit of detection in both groups (data not shown).

All these results with DHA supplemented mice are in accordance with those obtained in *FAT-1* mice and suggest that DHA prolongs the late inflammatory response, delaying its resolution.

To better explain which family of fatty acids is responsible for the findings of the present study, we separated C57black/6 mice into two groups: (1) orally supplemented with DHA-rich oil and (2) supplemented with DHA+LA (linoleic acid).

The results bellow showed, that when is administered LA together with DHA, there is an increase of LA incorporation in the skin lipid fractions of PC and PE with no alterations in DHA incorporation as well as, in the ω-6/ω-3 ratio. The elevated incorporation of LA in the skin, did not change the wound closure, proving that the worsening in the wound healing of FAT-1 and DHA supplemented mice is due the increase of DHA and not of reduction of ω-6 fatty acids **(Figure 6).**

Neutrophils and macrophages isolated from *FAT-1* mice had increased inflammatory responses

Considering that one-day after skin wound induction neutrophils are the prevalent cells at the wound site [13], we investigated whether there was any functional difference

between cells isolated from *FAT-1* and WT mice. For this, we used thioglycollate-elicited peritoneal neutrophils (**Supplemental Figure 2A)** and neutrophils obtained from bone marrow and isolated using a Percoll gradient (**Supplemental Figure 2D**).

We did not observe any difference in neutrophil recruitment to the peritoneal cavity in response to thioglycollate in *FAT-1* mice when compared to WT mice (**Supplemental Figures 2B and 2C**). On the other hand, there was an increase in TNF-α and a reduction (p=0.053) in IL-10 production by bone marrow-isolated neutrophils from *FAT-1* mice when compared to WT mice (**Supplemental Figure 2E**). No alterations were observed in phagocytosis index (data not shown).

There is a significant recruitment of macrophages to the wound site at the 3rd day after wounding [13]. Production of inflammatory mediators by macrophages isolated from the peritoneal cavity of *FAT-1* and WT mice, pre-stimulated or not with thioglycollate, which mimic the cells present at the 3rd day of wounding, was investigated (**Supplemental Figure 3A**). Macrophages isolated from *FAT-1* mice, following thioglycollate stimulation, exhibited higher production of TNF-α and lower production of IL-10 when in the presence of lipopolysaccharide (LPS), as compared to cells from WT mice (**Supplemental Figures 3B and 3C**). At the same time, resident peritoneal macrophages isolated from the *FAT-1* group showed higher TNF-α production without LPS stimulation (**Supplemental Figure 3E**).

Taken together, these results reinforce pro-inflammatory responses observed in *FAT-1* mice during wound healing.

Quality of repaired tissue is altered in *FAT-1* mice

To verify if the slow resolution of the inflammatory phase of the skin wound healing process impairs the tissue quality, we analysed the collagen fibre organization in skin wound tissue collected twenty-one days after wound induction. *FAT-1* mice exhibited fasciculated orientation of the collagen fibers and thicker epithelium, different from the WT mice, which

presented a more reticular organization of the collagen fibers, normal epithelium and hair follicles (**Figure 7**). These results indicate that the tissue repair was impaired in *FAT-1* mice.

DISCUSSION

In the present study, the high DHA content observed in *FAT-1* transgenic mice and mice supplemented with DHA-rich fish oil, slowed the resolution of the inflammatory phase and impaired the wound healing process.

Polyunsaturated fatty acids (PUFAs), such as those in the omega-6 (ω-6) and omega-3 (ω-3) family, have been the target of research related to inflammatory diseases, as they are considered modulating nutrients of this process [26].

Commonly, the typical western diet is rich in ω-6 fatty acids due to the abundance of linoleic acid (LA), an essential fatty acid present in corn, sunflower and safflower oils. As a result, ω-3 fatty acids represent only a small percentage of daily fat intake and are obtained from two main dietary sources: plants and fish [6].

After consumption, ω-6 and ω-3 fatty acids are incorporated into cell membranes, where they modulate membrane protein function, cell signaling and gene expression. Dietary ω-3 fatty acids compete with ω-6 fatty acids for incorporation, so that when the ratio of one increase, the incorporation of the other is reduced [6].

At skin, fatty acids alter the structural and immunological status since they interfere with maturation and differentiation of the stratum corneum and modulate the production of pro-inflammatory eicosanoids, reactive species (ROS and RNS), and cytokines, thus influencing the inflammatory response and possibly wound healing [27].

LA constitutes 40% of the fatty acids in the skin and plays an important role for its function [21]. In previously published studies from our group, a beneficial function of ω-6 in the skin wound healing process has been demonstrated [19, 21].

However, although the function of ω-6, such as LA, is clarified as promoting the skin wound healing, the effects of ω-3 are less clear. In the present study, we demonstrated that the

deleterious effects on wound healing were due to increased incorporation of DHA instead of the reduction on ω-6 fatty acids.

FAT-1 and DHA-fed groups showed an increase of inflammation. The elevated concentrations of CXCL-1 and CXCL-2 observed in *FAT-1* mice, indicate an uncontrolled inflammation promoting recruitment of leukocytes to the site of injury [28]. On the other hand, IL-10 minimizes the production of pro-inflammatory mediators and controls inflammation, being necessary for the late inflammatory phase [29]. The reduction of IL-10 production seen in skin wound tissue in *FAT-1* mice, was also seen for neutrophils and macrophages isolated from *FAT-1* mice, which had increased TNF-α production. All these observations are associated with the persistent inflammation in the skin wound tissue of *FAT-1* mice five days after wounding as indicated by increased TNF-α concentration, inflammatory cells and edema.

The DHA-fed group also had elevated TNF-α concentration in the late inflammatory phase. TNF-α is mainly produced 12 or 24 hours after wound induction and its levels return to baseline at the end of the proliferative phase of healing [29]. Initially, TNF-α production stimulates the recruitment of cells and the production of chemokines and growth factors. However, excessive TNF-α production is associated with chronic inflammation and tissue destruction [30-31].

All these inflammatory signals could be influenced by AA metabolism, which is related with homeostatic and pro-inflammatory events [32]. Although the increased production of eicosanoids derived from ω-3 FA may be associated with greater availability of these fatty acids in cellular membranes, the demand for eicosanoids from AA is higher due to the inflamed microenvironment [32].

There was an elevated concentration of eicosanoids derived from ω-3 FA in the DHA group. However, the concentrations were much lower than those of eicosanoids derived from

AA. Metabolites formed from ω-3 FA have lesser biological potency than those derived from ω-6 FA, and often compete for the same receptor, further dampening the biological effect of the latter [32].

The DHA group showed a higher concentration mainly of 18-HEPE, known to be a potent anti-inflammatory lipid mediator [33]. Studies have demonstrated that supplementation with fish oil increase this metabolite. In humans with chronic kidney disease, the increase of 18-HEPE limited inflammation [34]. The increase of 18-HEPE in brain tissue of *FAT-1* mice promoted remyelination [35]. In both *in vivo* and *in vitro* experiments with these transgenic mice, an 18-HEPE-rich environment prevented macrophage-mediated cardiac remodeling via cardiac fibroblasts [36]. Similarly, in a liver tumorigenesis study model, 18-HEPE was able to significantly decrease macrophages' TNF-α formation, suppressing the disease [33]. Another recent study with *FAT-1* mice showed an elevated 18-HEPE level in the serum as well as fewer pulmonary metastatic colonies, and reduction in TNF-α concentrations and in pulmonary MPO activity [37]. However, the concentration of 18-HEPE found in this study was 400 pg/mL and in the present study it was 20 pg/mg of tissue. Nevertheless, in the present study, the increase of 18-HEPE did not have a strong effect on cutaneous wound healing.

DHA-supplemented mice also had increased 5-HEPE, 11-HEPE and 16,17-EpDPE. 5-HEPE is one of the main metabolites produced from EPA by 5-lipoxygenase (5-LOX) and it is involved in many inflammatory processes. In endothelial cells, treatment with 5-HEPE activated the Keap1-Nrf2 pathway and upregulated the expression of enzymes that maintain the antioxidative capacity of the cells [38]. Interestingly, in a controversial study, a pro-inflammatory effect of DHA in an airway inflammation model was observed [39]. In this study, mice supplemented with DHA had elevated infiltration of eosinophils and

macrophages in the bronchoalveolar lavage, and increased production of IL-6. This inflammatory profile was associated with elevated DHA metabolites, like 16,17-EpDPE [39].

The role of eicosanoids and other lipid mediators derived from EPA and DHA in the cutaneous wound healing process is unclear and more studies are necessary to better characterize the effects of these metabolites on wound healing.

DHA-supplemented mice showed reduced concentrations of metabolites derived from AA. However, the concentrations of PGE_2 and PGD_2 were higher compared to those of all other metabolites. PGE_2 acts as an inflammatory mediator and a fibroblast modulator, improving tissue repair and regeneration, so that suppression of PGE_2 inhibits tissue regeneration and leads to excessive wound scar formation [40-41]. On the other hand, it was demonstrated that PGD_2 inhibited hair follicle neogenesis in the skin wound healing model, suggesting a deleterious effect on healing [42]. Therefore, the reduction of AA metabolites, due to the ω-3 FA-rich microenvironment in the late inflammatory phase, could promote an imbalance of required PGs at this stage, impairing skin wound healing.

The elevated inflammation did not impair the final wound closure, but in *FAT-1* mice, the quality of repaired tissue was altered, as demonstrated by the collagen reorganization and structural aspects.

Collagen is responsible for giving support to resident cells and it also plays an important role in inflammatory cell functions [43]. The most significant difference between normal tissue and wound tissue is the orientation of the fibrous matrix [44]. It is described that mice have a reticular orientation of collagen fibers in the basal condition, with the fascicular orientation mediating collagen remodeling transition during the last stages of the healing process [43]. Thus, the fascicular orientation exhibited by transgenic mice, indicates a less evolved healing process.

Additionally, it is known that the presence of hair follicles in the repaired tissue is associated with functional recovery [45]. Hair follicle neogenesis occurs during tissue regeneration, and, the absence of stimulus for this process determines the difference between scar-forming and regenerative skin wound healing [45]. Therefore, the presence of more hair follicles in the repaired skin tissue of WT mice corroborates that these animals are more advanced in healing than the *FAT-1* mice.

Taken together, these results suggest that the increased DHA content in the two experimental models slows the inflammatory phase resolution of wound repair and impairs the quality of healed skin tissue.

ACKNOWLEDGMENTS

The authors thank Gilson Murata and Fernando Moreira Simabuco for technical assistance. The authors acknowledge Professor Jing X. Kang for the provision of the *FAT-1* mice and Professor Rui Curi for the support and encouragement.

DECLARATIONS OF INTEREST

The authors state no conflict of interest.

FUNDING INFORMATION

This study was supported by a research grant from Fundação de Amparo à Pesquisa do Estado de São Paulo (FAPESP) grants 2013/06810-4; 2016/02021-3 and 2016/23298-3. The study was also financed by the National Council for Scientific and Technological Development (CNPq) and Coordenação de Aperfeiçoamento de Pessoal de Nível Superior - Brasil (CAPES) - Finance Code 001.

AUTHOR CONTRIBUTION STATEMENT

TC, MARV, and HGR designed the research. HGR, MARV, SRC, and PCC provided essential reagents and materials. TC, CMCK, BB, MBPdA, ARC, HLF, FCPM and EMS conducted the experiments. TC, CMCK, MAT, SRC and HGR analyzed the data. TC, CMCK, HGR, MARV, and PCC wrote the paper. TC, CMCK and HGR had the primary responsibility to prepare the final version of the paper. All authors have read and approved the final manuscript version.

REFERENCES

1. Jeffcoate W1; Bakker K. World Diabetes Day : footing the bill. *Lancet.* **365,** 1527 (2005).
2. Dickinson, L. E. & Gerecht, S. Engineered Biopolymeric Scaffolds for Chronic Wound Healing. *Front. Physiol.* **7,** (2016).
3. Serhan, C. N., Chiang, N. & Dalli, J. The Resolution Code of Acute Inflammation: Novel Pro- Resolving Lipid Mediators in Resolution. *Semin Immunol. 2015* **27,** 200–215 (2016).
4. Powell, D. *et al.* Chemokine signaling and the regulation of bidirectional leukocyte migration in interstitial tissues. *Cell Rep.* **19,** 1572–1585 (2017).
5. Eming, S. A., Martin, P. & Tomic-canic, M. Wound repair and regeneration : Mechanisms , signaling , and translation. *Sci Transl Med.* **6,** (2014).
6. Bradberry, J. C. & Hilleman, D. E. Overview of omega-3 Fatty Acid therapies. *P T* **38,** 681–91 (2013).
7. Calder, P. C. Functional Roles of Fatty Acids and Their Effects on Human Health. *J. Parenter. Enter. Nutr.* **39,** 18S–32S (2015).
8. Oikonomou, E. *et al.* Effects of omega-3 polyunsaturated fatty acids on fibrosis, endothelial function and myocardial performance, in ischemic heart failure patients. *Clin. Nutr.* **18,** 1–10 (2018).
9. Mello, A. H. De *et al.* Omega-3 Fatty Acids Attenuate Brain Alterations in High-Fat Diet-Induced Obesity Model. *Mol. Neurobiol.* **56,** 513–524 (2019).
10. Kim, H.-C., Jung, T. W., Abd El-Aty, A. M., Chung, Y. H. & Jeong, J. H. Protectin DX attenuates LPS-induced inflammation and insulin resistance in adipocytes via

AMPK-mediated suppression of the NF-κB pathway. *Am. J. Physiol. Metab.* **315,** E543–E551 (2018).

11. Chen, X. *et al.* Omega-3 polyunsaturated fatty acid attenuates the inflammatory response by modulating microglia polarization through SIRT1-mediated deacetylation of the HMGB1 / NF- κ B pathway following experimental traumatic brain injury. *J. Neuroinflammation* **15,** 1–15 (2018).

12. Pizato, N. *et al.* Omega-3 docosahexaenoic acid induces pyroptosis cell death in triple-negative breast cancer cells. *Sci. Rep.* **8,** 1–12 (2018).

13. Turk, H. F. *et al.* Inhibitory effects of omega-3 fatty acids on injury-induced epidermal growth factor receptor transactivation contribute to delayed wound healing. *Am. J. Physiol. Physiol.* **304,** C905–C917 (2013).

14. McDaniel, J. C., Belury, M., Ahijevych, K. & Blakely, W. Omega-3 fatty acids effect on wound healing. *Wound Repair Regen.* **16,** 337–345 (2008).

15. Arantes, E. L. *et al.* Topical Docosahexaenoic Acid (DHA) Accelerates Skin Wound Healing in Rats and Activates GPR120. *Biol. Res. Nurs.* **18,** 411–419 (2016).

16. Innes, J. K. & Calder, P. C. The Differential Effects of Eicosapentaenoic Acid and Docosahexaenoic Acid on Cardiometabolic Risk Factors : A Systematic Review. *Int. J. Mol. Sci.* **19,** 1–22 (2018).

17. Gorjão, R. *et al.* Comparative effects of DHA and EPA on cell function. *Pharmacol. Ther.* **122,** 56–64 (2009).

18. Stone, M. B. *et al.* Fat-1 mice convert n-6 to n-3 fatty acids. *Nature* **427,** 504 (2004).

19. Rodrigues, H. G., Vinolo, M. A., Magdalon, J., Vitzel, K. & Nachbar, R. T. Oral Administration of Oleic or Linoleic Acid Accelerates the Inflammatory Phase of Wound Healing. *J. Invest. Dermatol.* **132,** 209–15 (2012).

20. Fisk, H. L., West, A. L., Childs, C. E., Burdge, G. C. & Calder, P. C. The Use of Gas

Chromatography to Analyze Compositional Changes of Fatty Acids in Rat Liver Tissue during Pregnancy. *J. Vis. Exp.* 1–10 (2014). doi:10.3791/51445.

21. Rodrigues, H. G. *et al.* Oral Administration of Linoleic Acid Induces New Vessel Formation and Improves Skin Wound Healing in Diabetic Rats. *PLoS One* **11,** 1–19 (2016).

22. Bradford, M. M. *et al.* A rapid and sensitive method for the quantitation of microgram quantities of protein utilizing the principle of protein-dye binding. *Anal. Biochem.* **72,** 248–254 (1976).

23. Consonni, S. R. *et al.* Recovery of the pubic symphysis on primiparous young and multiparous senescent mice at postpartum. *Histol. Histopathol.* **27,** 885–896 (2012).

24. Quehenberger, O. *et al.* Lipidomics reveals a remarkable diversity of lipids in human plasma,. *J. Lipid Res.* **51,** 3299–3305 (2010).

25. Wang, Y., Armando, A. M., Quehenberger, O., Yan, C. & Dennis, E. A. Comprehensive ultra-performance liquid chromatographic separation and mass spectrometric analysis of eicosanoid metabolites in human samples. *J. Chromatogr. A* **1359,** 60–69 (2014).

26. Vodovotz, Y. *et al*. Translational Systems Approaches to the Biology of Inflammation and Healing. *Immunopharmacol Immunotoxicol* **32**, 181–195 (2010).

27. Silva, J. R. *et al*. Wound Healing and Omega-6 Fatty Acids: From Inflammation to Repair. *Mediators of Inflammation*, 2503950 (2018).

28. Armstrong, D. A., Major, J. A., Chudyk, A. & Hamilton, T. A. Neutrophil chemoattractant genes KC and MIP-2 are expressed in different cell populations at sites of surgical injury. *J. Leukoc. Biol.* **75,** 641–648 (2004).

29. Stanley, A. C. *et al.* Recycling endosome-dependent and -independent mechanisms for IL-10 secretion in LPS-activated macrophages. *J. Leukoc. Biol.* **92,** 1227–39 (2012).

30. Xu, F., Zhang, C. & Graves, D. T. Abnormal Cell Responses and Role of TNF-a in Impaired Diabetic Wound Healing. *Biomed Res. Int.* **2013,** 1–9 (2013).

31. Siqueira, M. *et al.* Impaired wound healing in mouse models of diabetes is mediated by TNF-α dysregulation and associated with enhanced activation of forkhead box O1 (FOXO1). *Diabetologia* **53,** 378–388 (2010).

32. Gabbs, M., Leng, S., Devassy, J. G. & Aukema, H. M. Advances in Our Understanding of Oxylipins Derived from Dietary PUFAs 1 , 2. *Adv Nutr* **6,** 513–540 (2015).

33. Weylandt, K. H. *et al.* Suppressed liver tumorigenesis in fat-1 mice with elevated omega-3 fatty acids is associated with increased omega-3 derived lipid mediators and reduced TNF- a. *Carcinogenesis* **32,** 897–903 (2011).

34. Barden, A. E. *et al.* The effect of n-3 fatty acids and coenzyme Q10 supplementation on neutrophil leukotrienes, mediators of inflammation resolution and myeloperoxidase in chronic kidney disease. *Prostaglandins Other Lipid Mediat.* **136,** 1–8 (2018).

35. Siegert, E., Paul, F., Rothe, M. & Weylandt, K. H. The effect of omega73 fatty acids on central nervous system remyelination in fat71 mice. *BMC Neurosci.* **18,** 1–9 (2017).

36. Endo, J. *et al.* 18-HEPE, an n-3 fatty acid metabolite released by macrophages, prevents pressure overload–induced maladaptive cardiac remodeling. *J. Exp. Med.* **211,** 1673–1687 (2014).

37. Li, J. *et al.* An omega-3 polyunsaturated fatty acid derivative, 18-HEPE, protects against CXCR4-associated melanoma metastasis. *Carcinogenesis* **39,** 1380–1388 (2018).

38. Nagahora, N., Yamada, H., Kikuchi, S., Hakozaki, M. & Yano, A. Nrf2 Activation by 5-lipoxygenase Metabolites in Human Umbilical Vascular Endothelial Cells. *Nutrients* **9,** 1–14 (2017).

39. Schuster, G. U. *et al.* Dietary Long-Chain Omega-3 Fatty Acids Do Not Diminish Eosinophilic Pulmonary Inflammation in Mice. *Am. J. Respir. Cell Mol. Biol.* **50,** 626–636 (2014).

40. Crunkhorn, S. Inhibiting prostaglandin breakdown triggers tissue regeneration. *Nat. Rev. Drug Discov.* **14,** 526 (2015).

41. Takeuchi, K. *et al.* Endogenous prostaglandin E 2 accelerates healing of indomethacin-induced small intestinal lesions through upregulation of vascular endothelial growth factor expression by activation of EP4 receptors. **25,** 67–74 (2010).

42. Nelson, A. M. *et al.* Prostaglandin D2 inhibits wound-induced hair follicle neogenesis through the receptor, Gpr44. *J Invest Dermatol.* **133,** 881–889 (2013).

43. Xue, M. & Jackson, C. J. Extracellular Matrix Reorganization During Wound Healing and Its Impact on Abnormal Scarring. *Adv. wound care* **4,** 119–136 (2015).

44. Fleischmajer, R. *et al.* Decorin Interacts with Fibrillar Collagen of Embryonic and Adult Human Skin. *J Struct Biol.* **106,** 82–90 (1991).

45. Lim, C. H. *et al.* Hedgehog stimulates hair follicle neogenesis by creating inductive dermis during murine skin wound healing. *Nat. Commun.* **9,** 1–13 (2018).

FIGURES

Figure 1

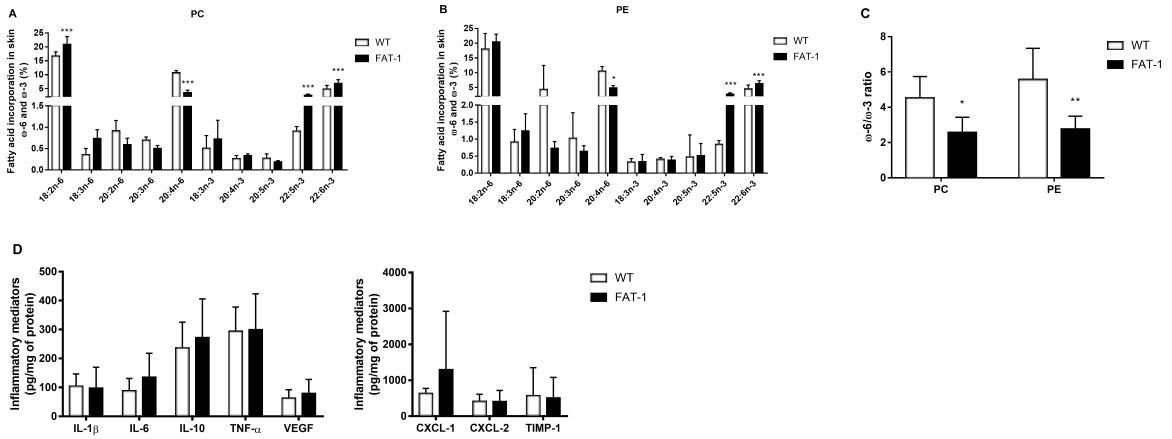

Figure 1. Fatty acid composition and inflammatory markers in skin unwounded tissue of WT and *FAT-1* mice. Percentage of ω-6 and ω-3 FAs and the ω-6/ω-3 FA ratio in phosphatidylcholine (PC) and phosphatidylethanolamine (PE) from unwounded skin tissue of WT and *FAT-1* mice, collected at the moment of skin wound induction (A, B, C). Inflammatory mediators were determined in the same tissues (D). The results are presented as mean ± SD. (*) $p<0.05$, (**) $p<0.01$ and (***) $p<0.001$ indicate statistically significant differences between WT and *FAT-1* mice. n = 5-12.

Figure 2

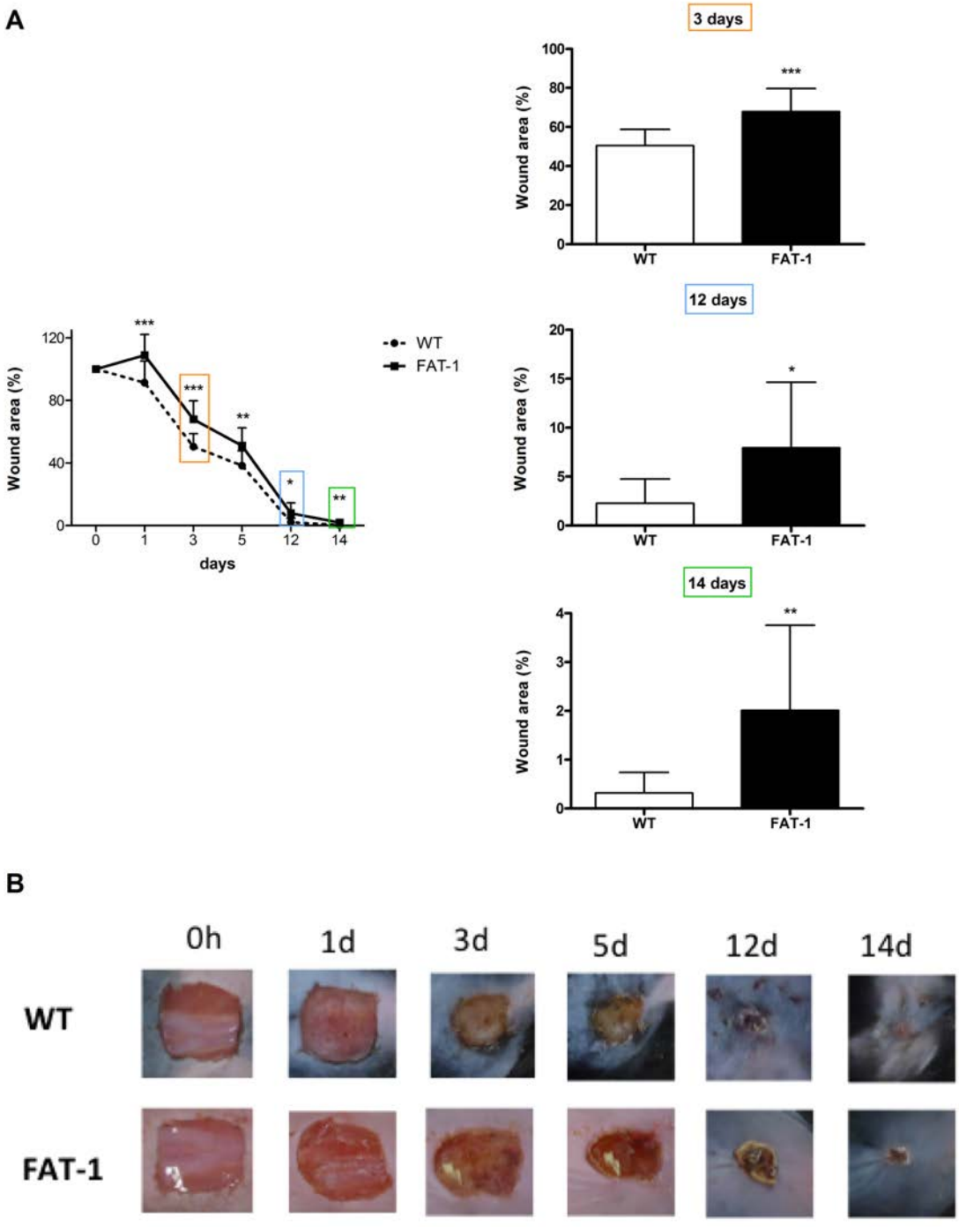

Figure 2. Skin wound closure in WT and *FAT-1* mice. Quantitative analysis (A) and representative images (B) of skin wound closure in WT and *FAT-1* mice. The skin wounds were followed for 14 days. The quantitative analysis was performed using the Image

J program. The results are presented as mean ± SD. (**) $p<0.01$ and (***) $p<0.001$ indicate statistically significant differences between WT and *FAT-1* mice. n = 8-16.

FIGURES

Figure 3

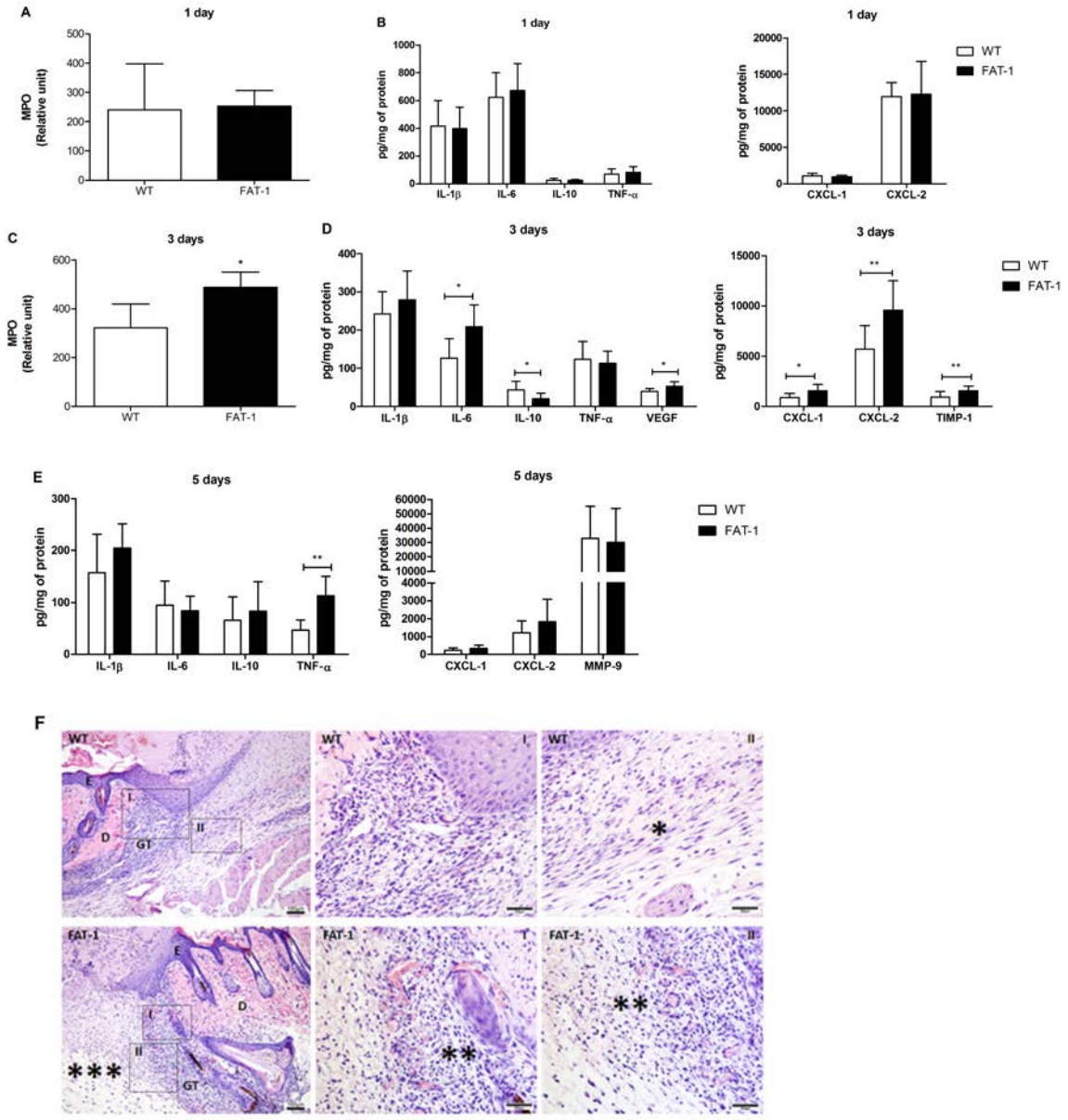

Figure 3. MPO activity, content of inflammatory mediators and histology of skin wound tissue of WT and *FAT-1* mice. MPO activity was measured in skin wound tissue of WT and *FAT-1* mice, collected one (A) and three days (C) after wounding. Content of inflammatory mediators were measured in skin wound tissue of one (B), three (D) and five days (E) from both groups. Histological sections of the skin wound tissue of five days from

both groups (F). In the first insets, H&E staining through representative light micrographs evidenced the morphology of the epidermis-E, dermis-D and granulation tissue-GT at the wound borders (Scale bar: 100 μm). The I and II insets (zoon images) in the WT group, represents the region with more organized and aligned tissue and few inflammatory cells. "*" indicates the alignment found at wound closure due to fibroblasts or myofibroblasts. In the *FAT-1* group, "**" indicates the presence of inflammatory cells and "***" represents edema with extravasation of cells and fluid water in the interstitium (Scale bar: 200 μm). The results are presented as mean ± SD. (*) $p<0.05$ and (**) $p<0.01$ indicate statistically significant differences between WT and *FAT-1* mice. n = 8-12.

Figure 4

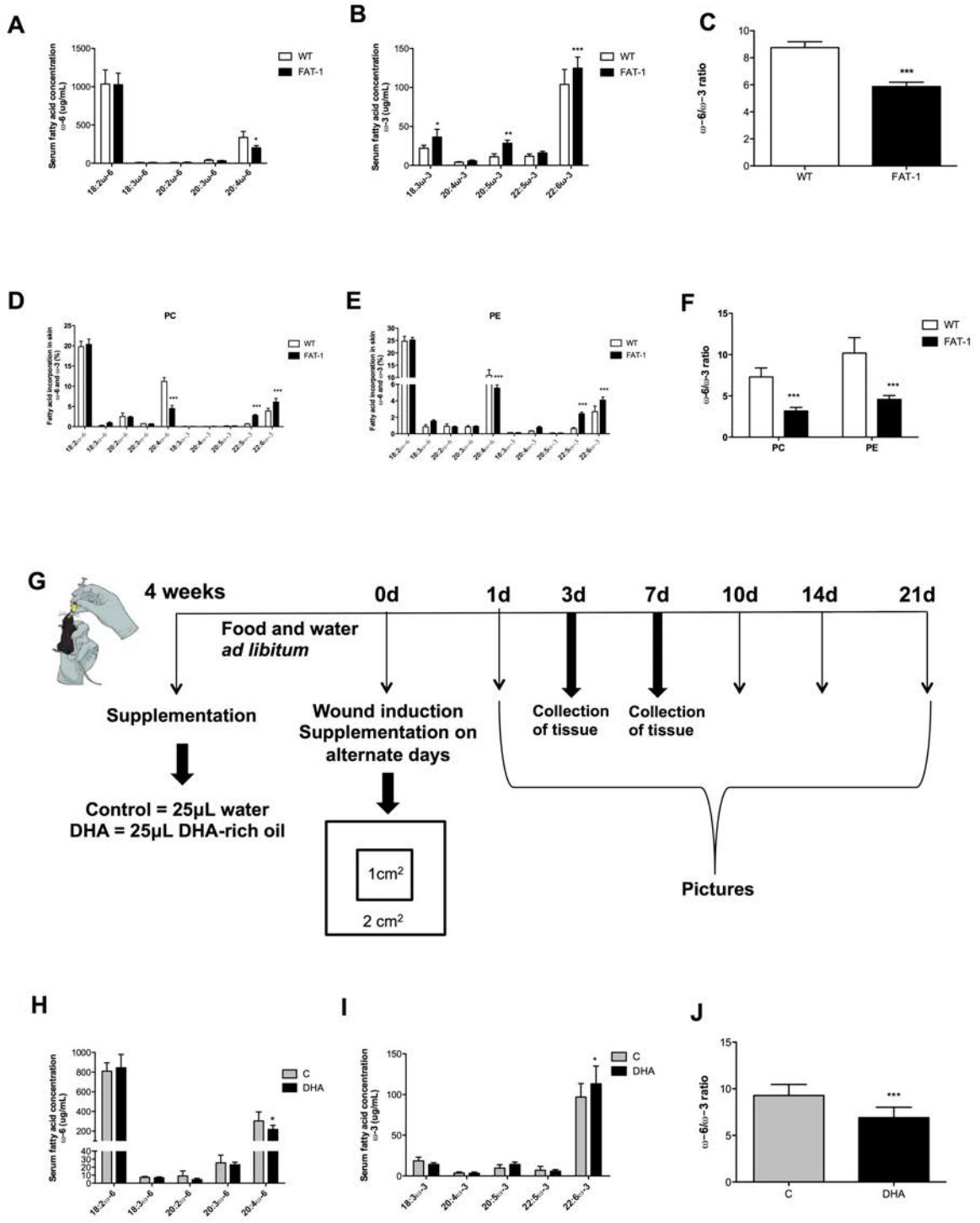

Figure 4. Fatty acid composition of serum and skin wound tissue three days after wounding. Concentrations of ω-6 and ω-3 FAs and the ω-6/ω-3 ratio in the serum from WT and *FAT-1* mice (A, B, C) and from mice supplemented with DHA-rich oil (H, I, J), collected three days after the skin wound induction. Percentage of ω-6 and ω-3 FAs and the ω-6/ω-3

ratio in skin phosphatidylcholine (PC) and phosphatidylethanolamine (PE) fractions from WT and *FAT-1* mice after three days of wounding (D, E, F). Experimental design of the supplementation with DHA-rich oil (G). The results were presented as mean ± SD. (*) $p<0.05$, (**) $p<0.01$ and (***) $p<0.001$ indicate statistically significant differences between WT and *FAT-1* and C and DHA mice. n = 5-8.

Figure 5

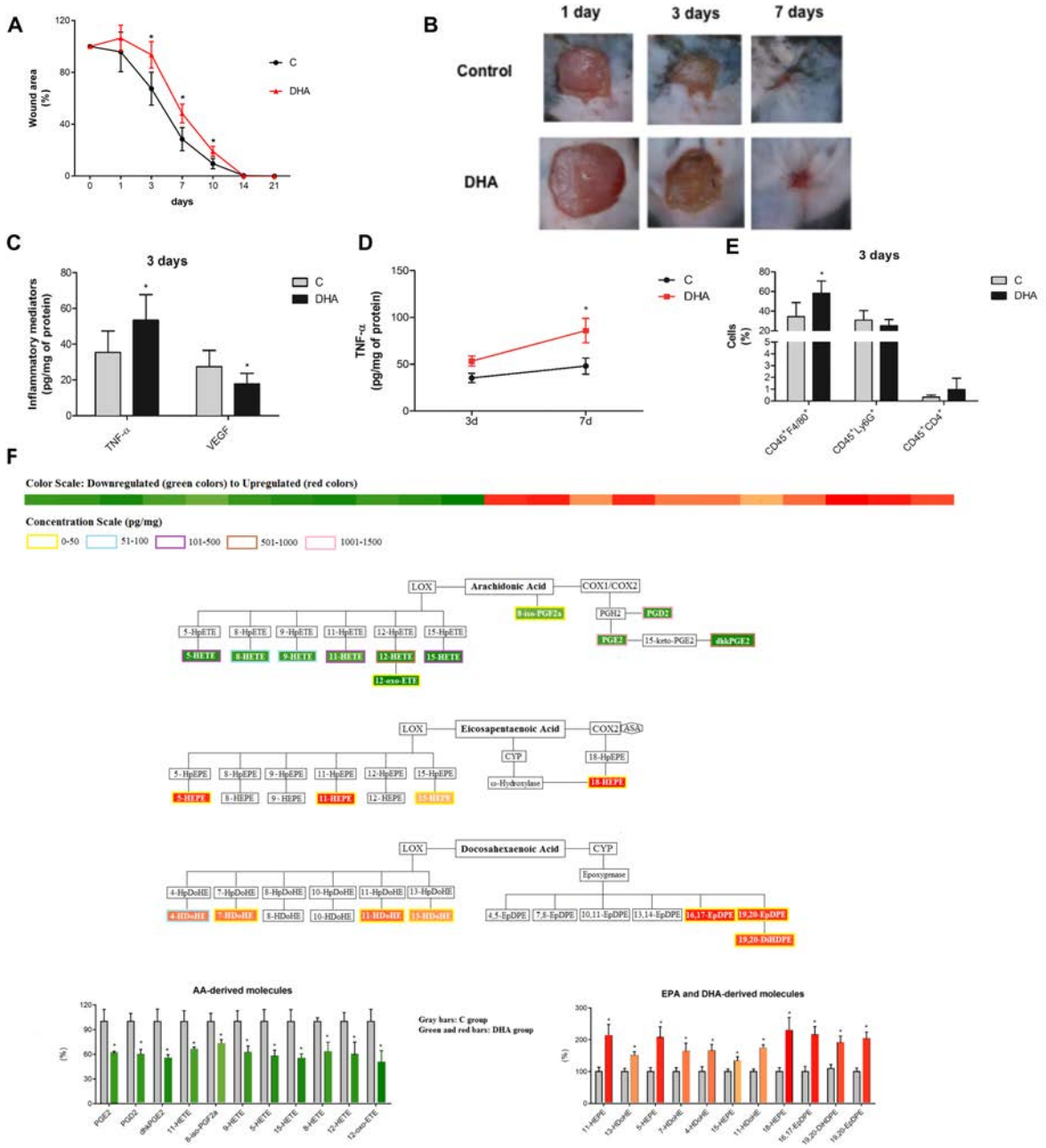

Figure 5. Wound closure time-course, inflammatory mediators, cells and eicosanoids content in skin wound tissue from control and DHA groups. Quantitative analysis (A) and representative images (B) of wound closure in the C and DHA groups. Skin wounds were followed for twenty-one days. Quantitative analysis was performed using the Image J program. Inflammatory mediators were quantified by ELISA in skin wound tissue of three and seven days from two groups (C, D). Cellular phenotyping was characterized by flow

cytometry in skin wound tissue of three days (E) and metabolites derived from AA, EPA and DHA were measure in the same wound time (F). The results were presented as mean ± SD. (*) $p<0.05$ indicate statistically significant differences between C and DHA mice. n = 3-8.

Figure 6

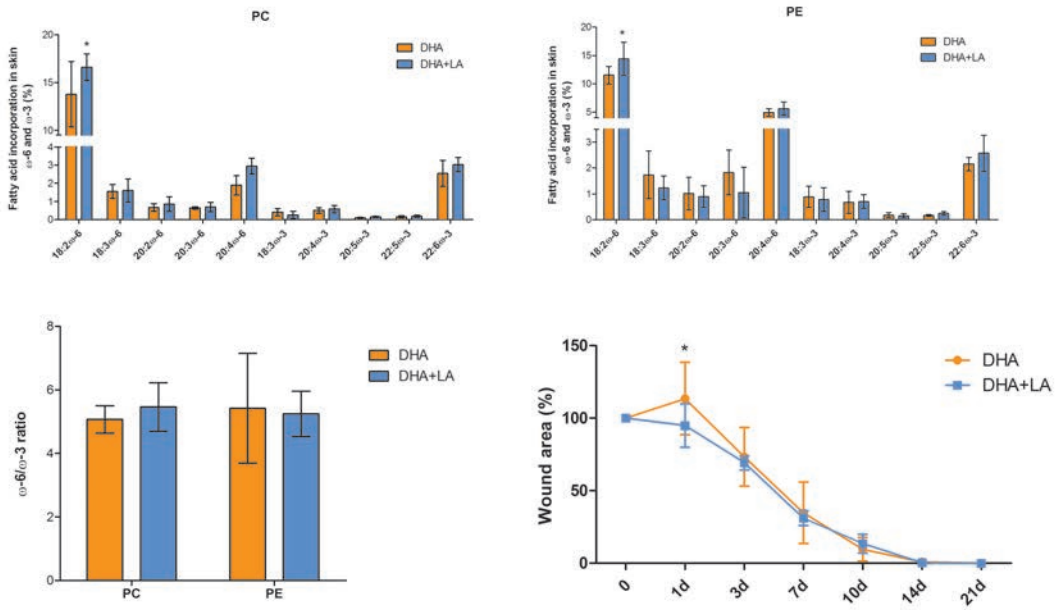

Figure 6 Lipid composition and wound closure. Percentage of ω-6 and ω-3 fatty acids and the ω-6/ω-3 ratio in phosphatidylcholine (PC) and phosphatidylethanolamine (PE) from unwounded skin tissue of mice supplemented with DHA and DHA+LA, collected at the moment of skin wound induction. These experiments were performed by gas chromatography. The wound closure was followed for 21 days after skin wound induction and analyzed by ImageJ program. The results are presented as mean ± SD. (*) $p<0.05$ indicate statistically significant differences between DHA and DHA+LA mice. n = 5 DHA and 8 DHA+LA.

Figure 7

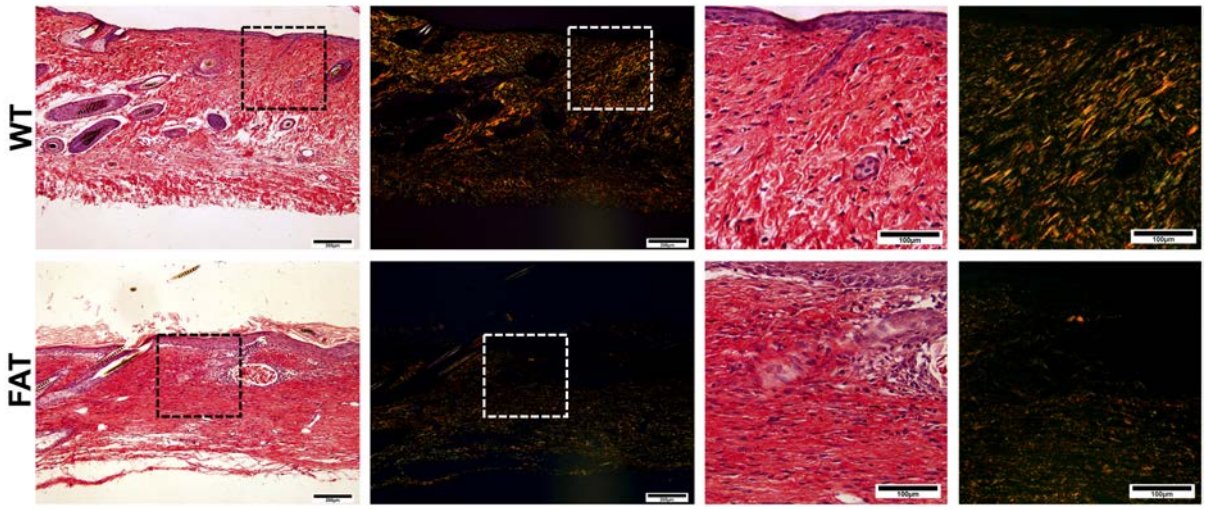

Figure 7. **Collagen reorganization and representative results in skin wound tissue of twenty-one days from WT and *FAT-1* mice.** Skin wound tissue of WT and *FAT-1* mice was collected after twenty-one days of wound induction and processed with Sirius Red and hematoxylin. Sirius Red staining and examination without (left) and with (right) polarized light revealed organization and maturation of collagen bundles. Scale bar: 200 μm and 100 μm (zoon images). n = 3-6.

SUPPLEMENTAL INFORMATION

Supplemental Table 1

Fatty acids	Sample 1 (%)	Sample 2 (%)	Sample 3 (%)
Methyl tetradecanoate	0.72	0.73	0.69
Hexadecanoic acid, methyl ester	2.21	2.21	2.14
9-Hexadecenoic acid, methyl ester, (Z)-	1.15	1.14	1.11
Methyl stearate	0.90	0.94	0.90
9-Octadecenoic acid, methyl ester, (E)-	2.91	2.97	2.78
9,12-Octadecadienoic acid (Z,Z)-, methyl ester	0.39	0.28	0.43
Eicosanoic acid, methyl ester	1.09	1.07	1.02
cis-11-Eicosenoic acid, methyl ester	1.88	1.87	1.80
cis-13-Eicosenoic acid, methyl ester	0.50	0.49	0.48
cis-11,14-Eicosadienoic acid, methyl ester	0.33	0.43	0.50
5,8,11,14-Eicosatetraenoic acid, methyl ester, (all-Z)-	1.16	1.19	1.13
5,8,11,14,17-Eicosapentaenoic acid, methyl ester, (all-Z)-	16.7	16.8	16.5
Docosanoic acid, methyl ester	0.73	0.68	0.71
13-Docosenoic acid, methyl ester, (Z)-	1.27	1.12	1.09
4,7,10,13,16,19-Docosahexaenoic acid, methyl ester, (all-Z)-	63.51	63.46	63.63
15-Tetracosenoic acid, methyl ester, (Z)-	4.54	4.58	5.01

Supplemental Table 1. DHA-rich oil composition. DHA-rich oil used for supplementation in the present study was analysed using a gas chromatograph-mass spectrometry. The experiment was performed in triplicate (sample 1-3).

Supplemental Figure 1

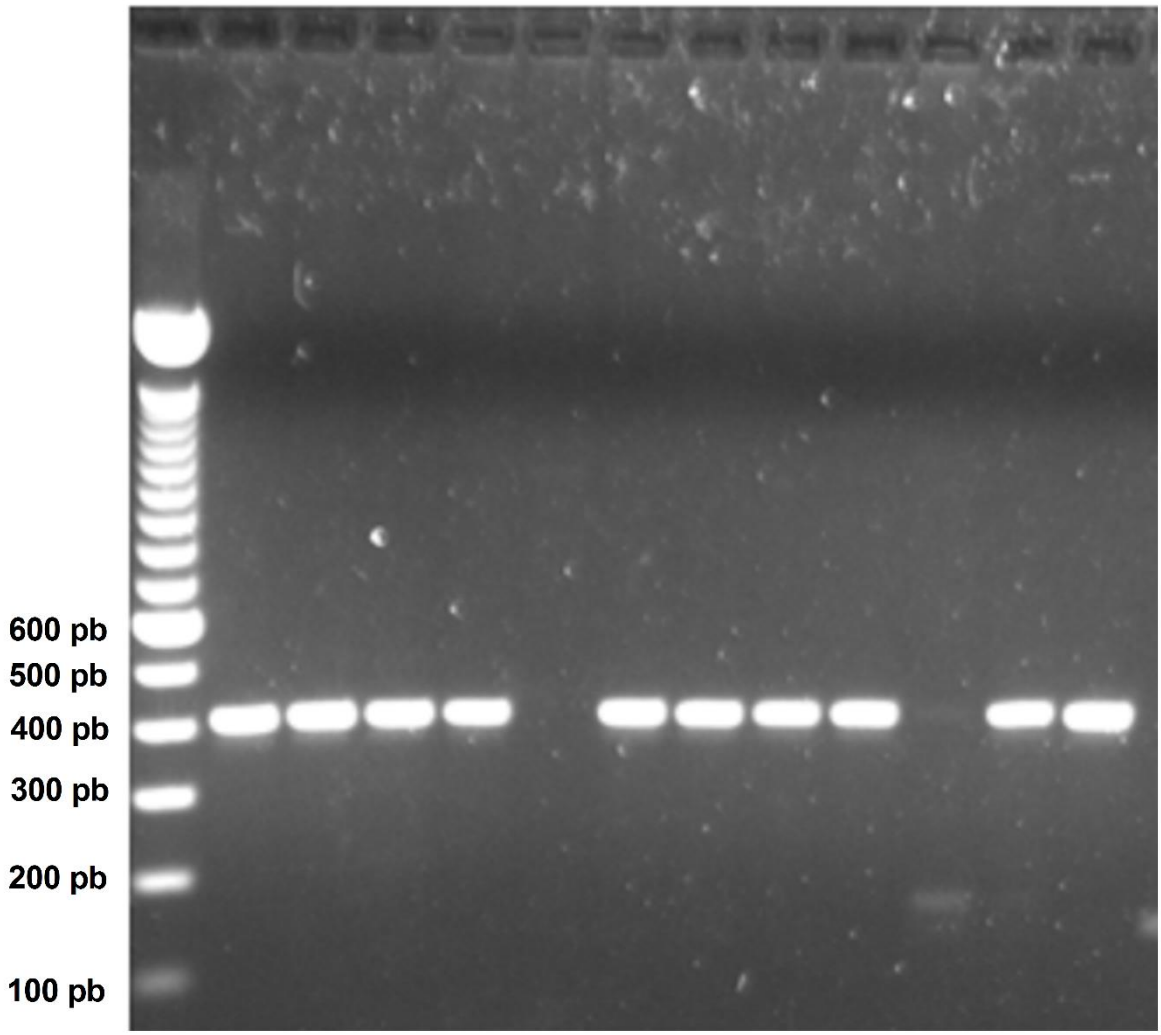

Supplemental Figure 1. Genotyping of WT and *FAT-1* mice. The white bands represent the *fat-1* gene amplified at molecular size 400 pb. The blank bands represent the WT mice.

Supplemental Figure 2

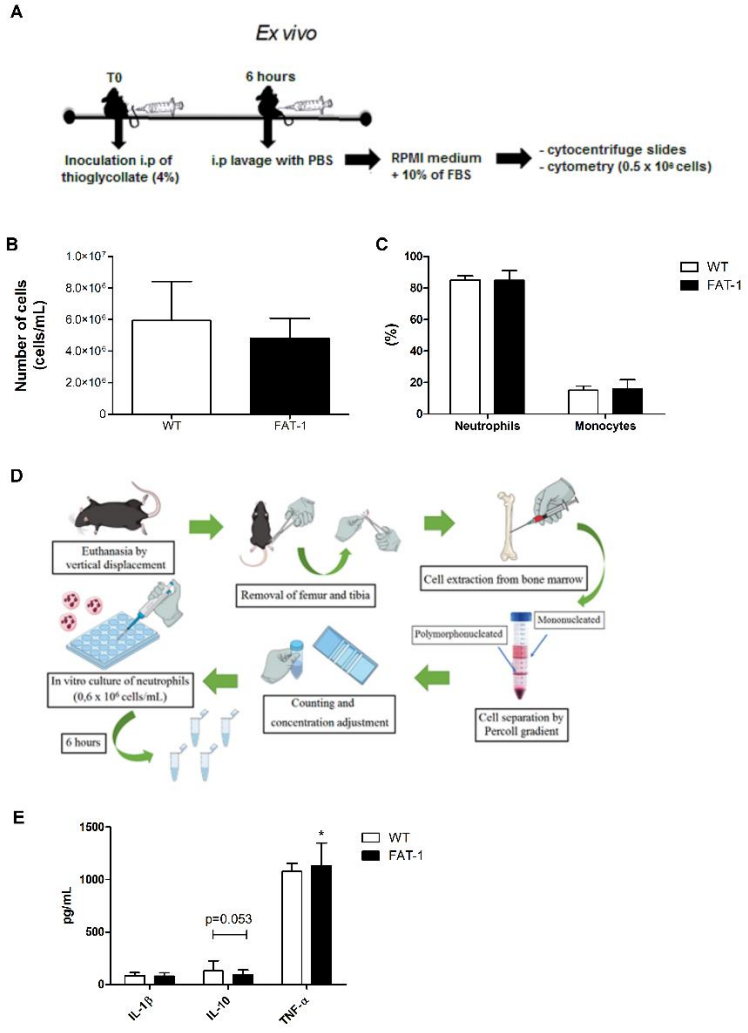

Supplemental Figure 2. Count and cytokine content of isolated cells from bone marrow and peritoneum of WT and *FAT-1* mice. Experimental design of intraperitoneal cells obtained after thioglycollate elicitation in WT and *FAT-1* mice (A) and counted by cytocentrifuge (B, C). Experimental design of cells isolated from bone marrow of WT and *FAT-1* mice and separated through a Percoll gradient (D). After counting, neutrophils from bone marrow were plated (0.6 x 10^6 cells/mL) and the supernatant collected after 6 hours of incubation for cytokines measurement by ELISA method (E). The results are presented as mean ± SD. (*) $p<0.05$ indicate statistically significant differences between WT and *FAT-1* mice. n = 4-11.

Supplemental Figure 3

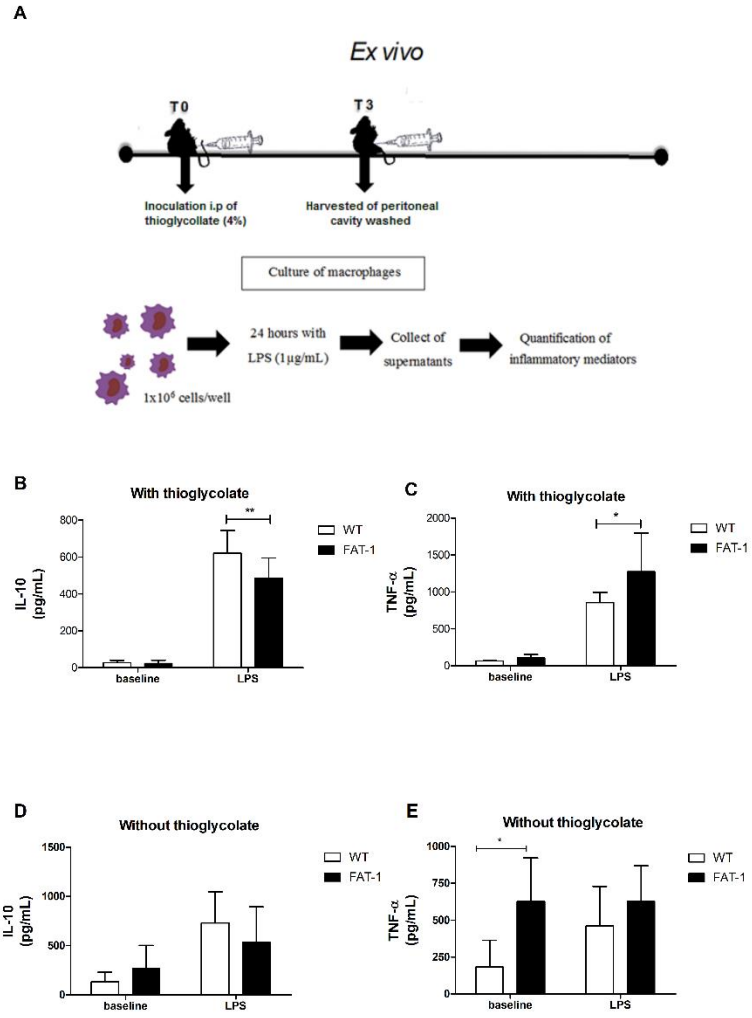

Supplemental Figure 3. Production of inflammatory mediators by cultured macrophages isolated from WT and *FAT-1* mice. Experimental design of isolation and culture of macrophages from WT and *FAT-1* mice (A): a thioglycollate solution (4%) was injected into the peritoneum of the WT and *FAT-1* group three days after skin wounding. The peritoneal fluid was collected and cells isolated by centrifugation; cells were counted, plated and cultured in medium with and without LPS (1 mg/mL). Cytokines were quantified in supernatants of cultured macrophages from mice treated with (B, C) or without thioglycolate (D, E) in baseline condition or with LPS stimulation (1 mg/mL). The results are presented as

mean ± SD. (*) $p<0.05$ and (**) $p<0.01$ indicate statistically significant differences between WT and *FAT-1* mice. n = 5-8.

Supplemental Figure 4

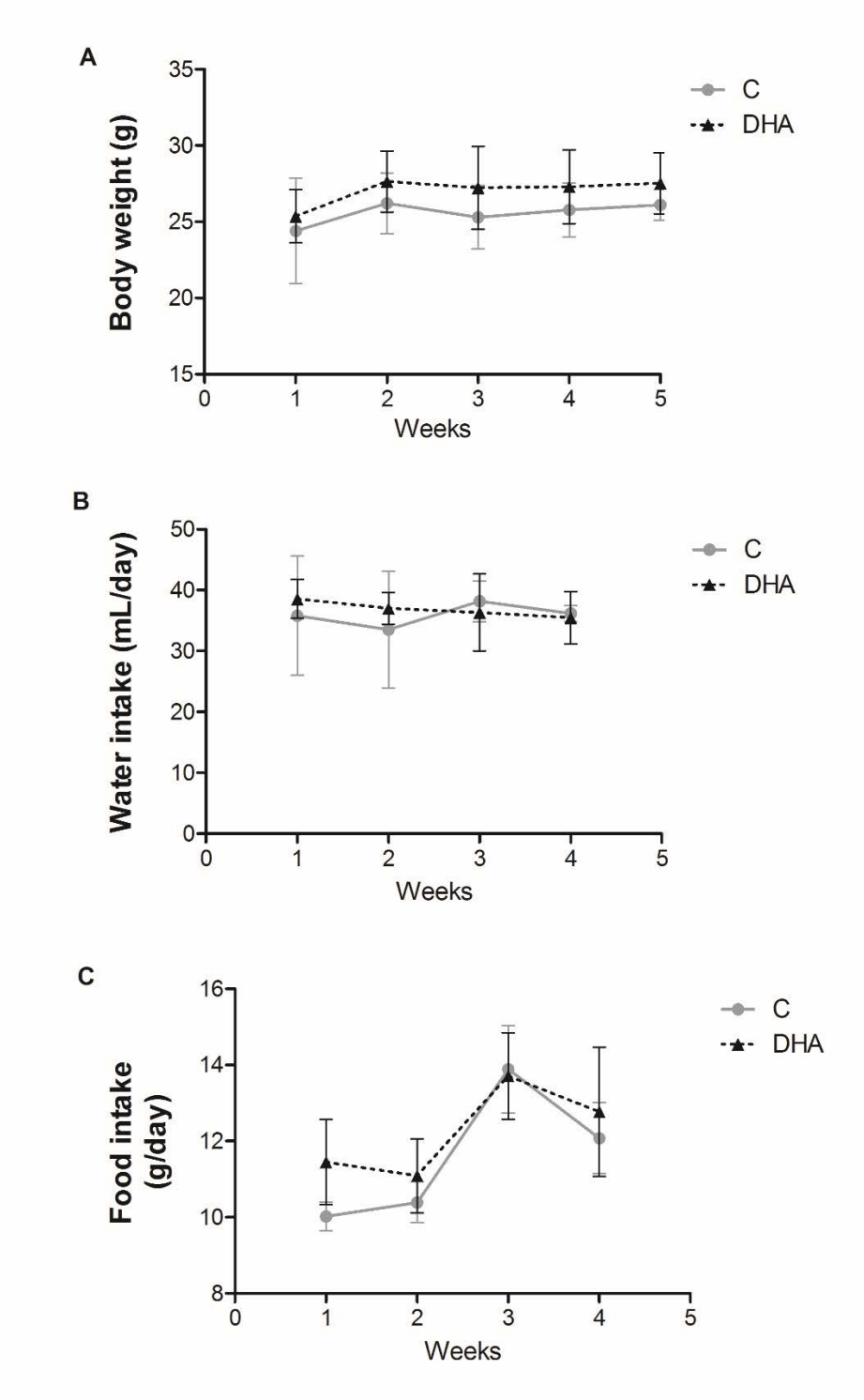

Supplemental Figure 4. Nutritional parameters of control mice and mice supplemented with DHA-rich fish oil. Control mice and mice supplemented with DHA-rich fish oil were followed for 5 weeks. The weight (A), water intake (B) and food intake (C) were measured. The results were presented as mean ± SD. n = 3-5.

Supplemental Figure 5

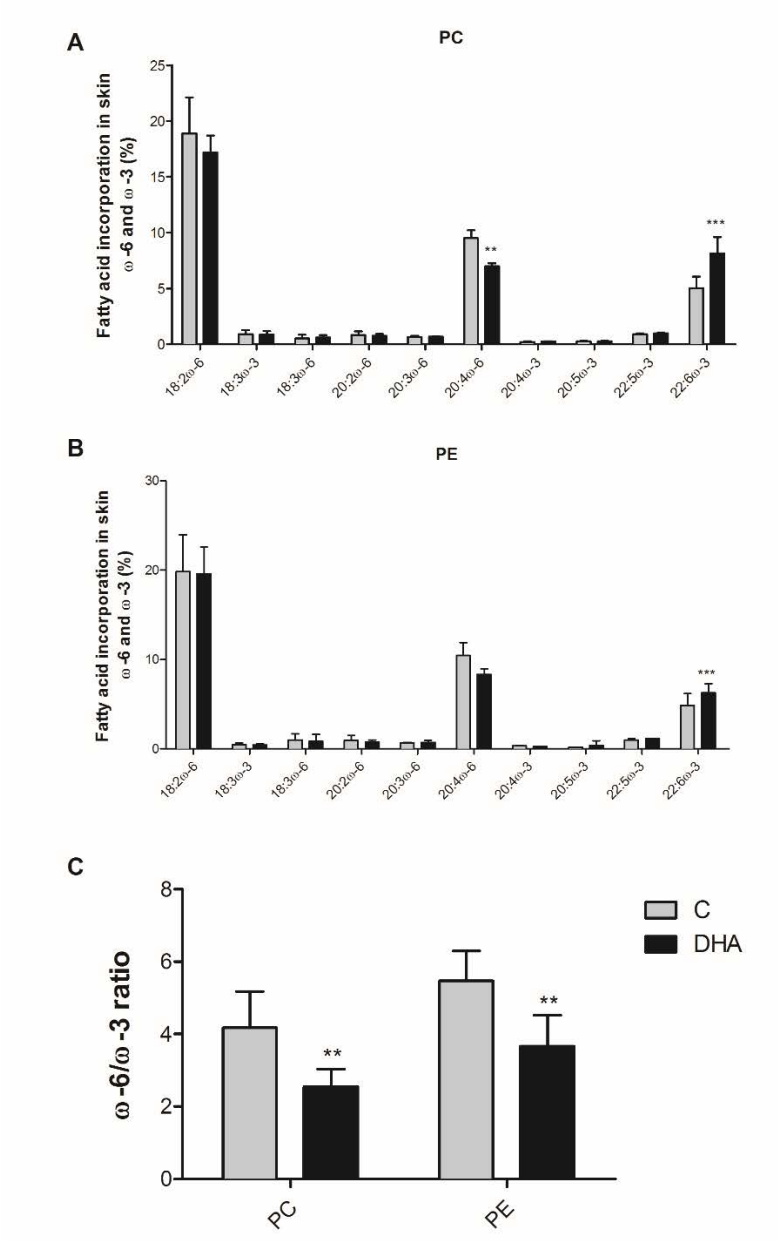

Supplemental Figure 5. Fatty acids composition of skin unwounded tissue collected from control mice and mice supplemented with DHA-rich fish oil. Percentage of ω-6 and ω-3 PUFAs in phosphatidylcholine (PC) (A) and phosphatidylethanolamine (PE) (B) and the ω-6/ω-3 PUFA ratio (C) from skin unwounded tissue of the C and DHA groups, collected at the moment of skin wound induction. The results were presented as mean ± SD. (**) $p<0.01$ and (***) $p<0.001$ indicate statistically significant differences between C and DHA mice. n = 6 animals per group.

Supplemental Figure 6

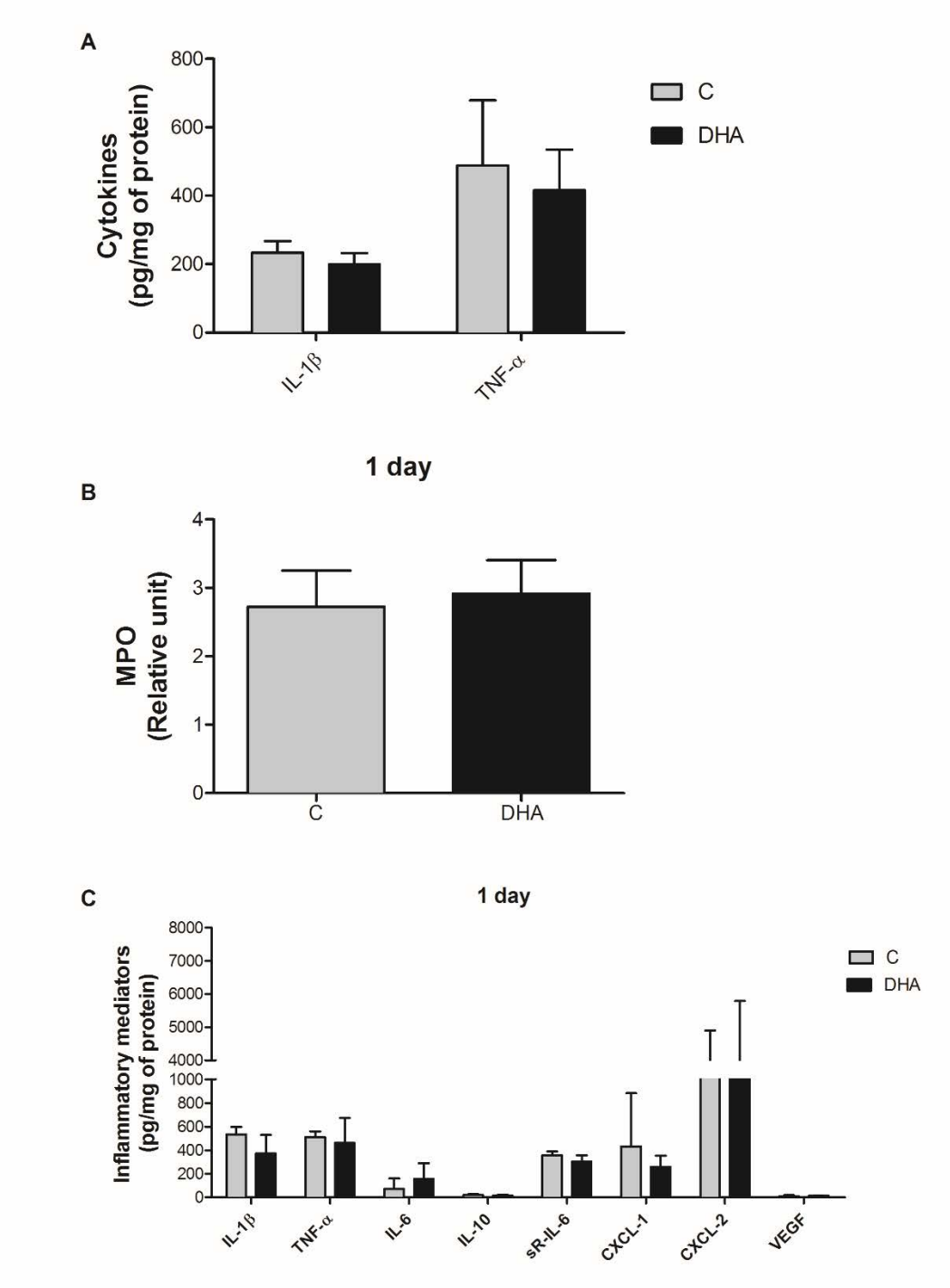

Supplemental Figure 6. MPO activity and content of inflammatory mediators in skin unwounded and wound tissues of one day period. Inflammatory mediators were quantified in unwounded (A) and skin wound tissue of one day period (C) from C and DHA mice by ELISA. MPO activity was measured only in skin wound tissue collected one day

after wound induction from both groups (B). The results were presented as mean ± SD. n = 3-8.